The Photocatalytic Activities of Tin(IV) Oxide-Surface Modified Titanium (IV) Dioxide Show a Strong Sensitivity to the TiO2 Crystal Form

Journal:	*The Journal of Physical Chemistry*
Manuscript ID:	jp-2012-02493f
Manuscript Type:	Article
Date Submitted by the Author:	14-Mar-2012
Complete List of Authors:	Tada, Hiroaki; Kinki University, Department of Applied Chemistry Fujishima, Musashi; Kinki University, School of science and engineering Jin, Qiliang; Kinki University, Department of Applied Chemistry Nolan, Michael; Tyndall National Institute, Electronics Theory Group Iwaszuk, Anna; Tyndall National Institute, Electronics Theory Group

The Photocatalytic Activities of Tin(IV) Oxide-Surface Modified Titanium (IV) Dioxide Show a Strong Sensitivity to the TiO_2 Crystal Form

Qiliang Jin,[a] Musashi Fujishima,[a] Michael Nolan,[b]* Anna, Iwaszuk[b], Hiroaki Tada [a]*

[a] Department of Applied Chemistry, School of Science and Engineering, Kinki University, 3-4-1, Kowakae, Higashi-Osaka, Osaka 577-8502, Japan

[b] Tyndall National Institute, Lee Maltings, University College Cork, Cork, Ireland

RECEIVED DATE (automatically inserted by publisher); h-tada@apch.kindai.ac.jp, michael.nolan@tyndall.ie

Supporting Information

ABSTRACT: The surface modification of rutile TiO_2 with extremely small SnO_2 clusters gives rise to a great increase in its UV-light-activity for the degradations of model organic water pollutants, while the effect is much smaller for anatase TiO_2. This crystal form-sensitivity is rationalized in terms of the difference in the electronic modification of TiO_2 through the interfacial Sn-O-Ti bonds. The increase in the density of states near the conduction band minimum of rutile by the hybridization with the SnO_2 cluster levels intensifies the light absorption, but this is not seen with modified anatase. The electronic transition from the valence band to the conduction band causes the bulk-to-surface interfacial electron transfer to enhance the charge separation. Further, the electrons relaxed to the conduction minimum are smoothly transferred to O_2 due to the action of the SnO_2 species as an electron transfer promoter.

INTRODUCTION

TiO_2 is the most promising "eco-catalyst" for environmental purification owing to its high oxidation power, high physicochemical stability, relative abundance in nature, and nontoxicity.[1,2] Usually, TiO_2 takes the crystal forms of anatase and rutile. For the degradation of organic pollutants, anatase is known to exhibit higher photocatalytic activity than rutile.[3] Moreover, the photocatalytic activity of TiO_2 has been revealed to strongly depend on not only the bulk structure but also the surface structure.[4] Thus, rational design of the surface electronic structure of TiO_2 brings the possibility of improvements in its photocatalytic activity. A new effective approach for that is the surface modification of TiO_2 with metal oxide clusters. To date, the visible-light-activation of TiO_2 has been achieved by the surface modification with oxides of transition metals including Cr,[5] Fe,[6-10] Ni,[11] and Cu.[12,13] Key to this surface modification is the dispersion state of the metal oxides on the TiO_2 surface[9] in the same manner as the doped system.[14] The chemisorption-calcination cycle (CCC) technique, where metal complexes are adsorbed *via* strong chemical bonds, and the organic part is oxidized by postheating, enables formation of molecule-sized metal oxide clusters on the TiO_2 surface in a highly dispersed state.[15] More recently, we have reported that the surface modification of anatase TiO_2 with molecular SnO_2 clusters by the CCC technique increases the UV-light-activity.[16] These surface modification effects are presumed to be sensitive to both the bulk and surface structures of TiO_2; however, further work in this area is required.

Herein we show that the tin oxide-surface modification of rutile (SnO_2/rutile) greatly increases the UV-light-activity, while the enhancing effect is small for anatase (SnO_2/anatase). This striking difference is discussed on the basis of the spectroscopic and electrochemical experiments and first principles density functional theory (DFT) simulations.

EXPERIMENTAL SECTION

Catalyst preparation. SnO_2 clusters were formed on the surfaces of rutile (mean particle size, d = 100 nm, TAYCA) and

anatase (d = 150 nm, A-100, Ishihara Sangyo) by the chemisorption-calcination cycle (CCC) technique using $[Sn(acac)_2]Cl_2$ as a precursor. After TiO_2 particles (1 g) had been added to 50 mL of a $[Sn(acac)_2]Cl_2$ ethanol solution, they were allowed to stand for 24 h at 298 K. The $[Sn(acac)_2]Cl_2$ concentration was changed from 1.0×10^{-3} M to 1.0×10^{-5} M. The solid samples were separated by centrifugation and washed twice with the solvent for the physisorbed complexes to be removed. Then, they were dried in vacuum at room temperature, followed by heating in air at 873 K for 1 h. For electrochemical measurements, mesoporous TiO_2 nanocrystalline film electrodes were used. An aqueous paste of the rutile paritlces (water = 3 : 7 w/w) was prepared by mixing in a agate mortar with a slight amount of ethanol added. The resulting paste was coated on F:SnO_2-film coated glass substrates (sheet resistance = 12 Ω/□) by a squeegee method. After drying in air, the sample was heated in air at 873 K to form nanocrystalline TiO_2 films (rutile/FTO).

Catalyst characterization. The Sn loading amount was determined by inductively coupled plasma spectroscopy (ICPS-7510, Shimadzu). The sample (0.02 g) was dispersed to hot conc. H_2SO_4 (5 mL), and the deposits were thoroughly dissolved into the solution by stirring. The solution was diluted 3 times in volume with water, and then the Sn concentration was measured. UV-vis diffuse reflectance spectrum of SnO_2/TiO_2 was recorded on a Hitachi U-4000 spectrophotometer. The spectrum was converted to the absorption spectrum by using the Kubelka-Munk function. Transmission electron microscopic (TEM) observation and energy dispersive X-ray (ED) spectroscopic measurements were performed using a JEOL JEM-3000F and Gatan Imaging Filter at an applied voltage of 300kV. X-ray photoelectron spectroscopic (XPS) measurements were performed using a Kratos Axis Nova X-ray photoelectron spectrometer with a monochromated Al K_α X-ray source ($h\nu$ = 1486.6 eV) operated at 15 kV and 10 mA. The take-off angle was 90º, and multiplex spectra were obtained for Sn_{3d}, O_{1s}, and Ti_{2p} photopeaks. All the binding energies were referenced with respect to the C_{1s} at 284.6 eV. The photoluminescence spectra were measured with an excitation wavelength of 320 nm at 77 K using a JASCO FP-6000 spectrofluorometer. The electrochemical properties of the SnO_2-surface modified TiO_2/FTO electrodes (SnO_2/TiO_2/FTO) were measured in 0.1 M $NaClO_4$ aqueous solution in a regular three-electrode electrochemical cell using a galvanostat/potentiostat (HZ-5000, Hokuto Denko). Glassy carbon and an Ag/AgCl electrode (TOA-DKK) were used as a counter electrode and a reference electrode, respectively.

Photocatalytic activity evaluation. SnO_2/TiO_2 particles (0.1 g) was added to 50 mL of 1.0×10^{-5} M 2-naphthol (2-NAP) solution (solvent, acetonitrile : water = 1 : 99 v/v) in a borosilicate glass container. The suspension was placed in the reaction cells, and then irradiated with a Xe lamp (Wacom HX-500) through two pieces of FTO-coated glass and a band-pass filter (33U, SIGMA KOKI CO., LTD.) transmitting the light of $330 < \lambda < 400$ nm for the UV-light photocatalytic activity evaluation and through a cut off filter (L-42 (Toshiba) transmitting the light of $\lambda > 400$ nm for the visible-light activity evaluation. Three mL of the solution was sampled every 5 min (UV) or 15min (Vis), and the electronic absorption spectra of the reaction solutions were measured using a spectrometer (UV-1800, Shimadzu) to determine the 2-NAP concentration from the absorption peak at 224 nm. A 596 ppm standard CH_3CHO gas (CH_3CHO/N_2) was introduced into a reaction vessel made of borosilicate glass (393 mL) to be diluted with air such that its initial concentration becomes ca. 285 ppm. After the adsorption equilibrium of CH_3CHO on SnO_2/TiO_2 particles (0.1 g) had been achieved under dark conditions, irradiation of UV- and visible-light ($\lambda > 290$ nm) was carried out at room temperature. The concentration of CH_3CHO was determined as a function of time by GC-FID-Methanizer (GC-FID: gas chromatography (GC-2014, Shimadzu), Methanizer (MTN-1, Shimadzu)) with a Porapak-Q column (3.0 mmϕ × 3.0 m): injection and column temperatures were 423 K and 393 K, respectively, and N_2 was used as a carrier gas.

DFT simulations. For the calculations of surface modified TiO_2 we use the DFT approach with corrections for on-site Coulomb interactions, DFT+U to describe consistently Fe and Ti oxidation states; no such correction is applied to SnO_2, since DFT adequately describes this system. For modeling TiO_2 rutile (110) and anatase (001) surfaces, we use a three dimensional periodic slab model within the VASP code.[17] The valence electrons were described by a plane wave basis set and the cut-off for the kinetic energy is 396 eV. There are 4 valence electrons for Ti, 8 for Fe, 4 for Sn and 6 for O. The exchange-correlation functional was approximated by the Perdew-Wang 91[18] functional. The Monkhorst-Pack scheme was used for K-point sampling with a (2×1×1) sampling grid. To describe Ti 3d states the DFT+U approach was used where U=4.5 eV. The need to

introduce U parameter in order to describe properly electronic states of d shells is well known.[19,20] Fe 3d states were described with U=6.5eV and J=1eV which are typical values from the literature.[21] For Sn, the electronic states are consistently described by DFT so no U correction was applied. The DFT+U approach gives relatively correct d state description but still gives an underestimation of the band gap and this depends on the precise DFT+U set up. We are aware of this important issue but are primarily concerned with qualitative changes in the band gap upon surface modification. With this in mind, the simulation results are important for understanding the experimental results. The rutile (110) surface is terminated by two coordinated bridging oxygens and the surface contains 5-fold and 6-fold coordinated Ti atoms. The anatase (001) surface is terminated by two coordinated oxygen atoms while the oxygen atoms in the surface are three coordinated. The Ti atoms in the surface are 5-fold coordinated. All surfaces have 12Å vacuum gap. We used a (4×2) surface supercell for both surfaces. For the consistency in the calculation we applied the same supercell for bare TiO_2 surface and free clusters.

The clusters are positioned on the TiO_2 surfaces and adsorption energy is computed from:

$$E^{ads} = E((MO_x)\text{-}TiO_2) - \{ E(MO_x) + E(TiO_2) \} \quad (1)$$

Where

$E((MO_x)n\text{-}TiO_2)$ = total energy of the MO_x cluster supported on the TiO_2 surface

$E(MO_x)$ and $E(TiO_2)$= total energies of the free MO_x cluster and the bare surface.

RESULTS AND DISCUSSION

SnO_2 clusters were formed on the surfaces of rutile and anatase by the CCC technique using $[Sn(acac)_2]Cl_2$ as a precursor.[16] The adsorption isotherms of $[Sn(acac)_2]Cl_2$ on rutile and anatase apparently exhibit Langmuir behavior (Figure S1 in SI). This adsorption proceeds via the ion-exchange between the complex ions and H^+ released from the surface Ti-OH groups.[16] The saturated adsorption amount and equilibrium constant were determined to be 0.29 ions nm^{-2} and 1.7×10^4 M^{-1} for anatase and 0.10 ions nm^{-2} and 4.6×10^4 M^{-1} for rutile, respectively. After the postheating of the complex-adsorbed TiO_2, no particle was observed on the rutile and anatase surfaces by transmission electron microscopy. Also, the oxidation state of Sn in the tin oxide species was confirmed to be 4+ by X-ray photoelectron spectroscopy. Clearly, extremely small SnO_2 clusters are formed on the TiO_2 surfaces by the CCC technique. The loading amount of Sn is expressed by the number of Sn ions per unit TiO_2 surface area (Γions nm^{-2}).

Figure 1 compares UV-vis absorption spectra of (A) SnO_2/anatase and (B) SnO_2/rutile. Anatase and rutile have strong absorption at $\lambda < 385$ nm and $\lambda < 410$ nm due to the interband electronic transition. In spectra (A), no spectral change is observed with the surface modification. On the other hand, in spectra (B), the absorption intensity increases, whereas the absorption edge is almost invariant. This indicates an enhancement of light absorption but without the band gap narrowing that was observed in the FeO_x/TiO_2[9,22] and NiO/TiO_2[11] systems.

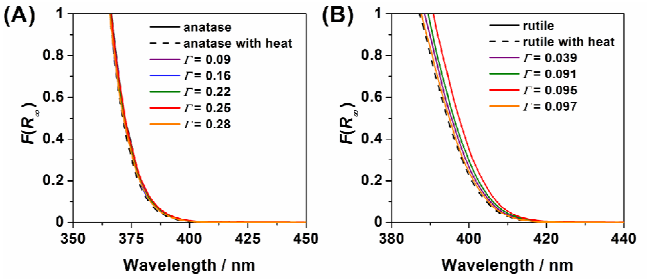

Figure 1. UV-Vis absorption spectra of (A) SnO_2/anatase and (B) SnO_2/rutile.

The photocatalytic degradation of 2-naphthol (2-NAP) was examined under illumination of UV-light ($330 < \lambda < 400$ nm, $I_{320\text{-}400\ nm} = 1.5$ mW cm^{-2}) and visible-light ($\lambda > 400$ nm, $I_{420\text{-}485\ nm} = 1.0$ mW cm^{-2}). 2-NAP, the starting material of azo-dyes, can be used as a model water pollutant to evaluate photocatalytic activity, since it has no absorption at $\lambda > 330$ nm.[23] UV-light irradiation of SnO_2/TiO_2 led to degradation of 2-NAP apparently obeying first-order kinetics. Figure 2A shows the first-order pseudo-rate constants for anatase (k_{UV}(A), blue circle) and rutile (k_{UV}(R), red circle) as a function of Γ. The SnO_2-surface modification of anatase has only a small positive effect on its photocataltyic activity. In contrast, k_{UV}(R) greatly increases with increasing Γ.

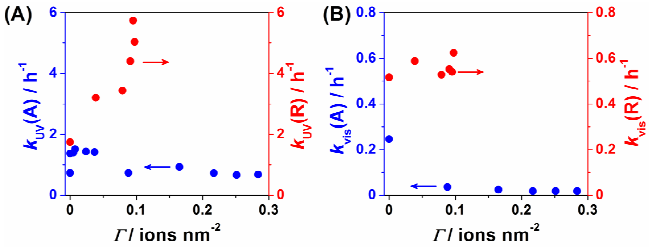

Figure 2. (A) Pseudo-rate constants of the 2-NAP degradation under UV-light irradiation for anatase (k_{UV}(A), blue circle) and rutile (k_{UV}(R), red circle) as a function of Γ. (B) Pseudo-rate constants of the 2-NAP degradation under visible-light irradiation for anatase (k_{vis}(A), blue circle) and rutile (k_{vis}(R), red circle) as a function of Γ.

Similar results were obtained also for the degradation of acetaldehyde used as a model air pollutant (Figure S2 in SI). Under visible-light irradiation, anatase and rutile show a low activity for the 2-NAP degradation. Figure 2 B shows the rate constants for 2-NAP degradation under visible light irradiation for anatase (k_{vis}(A), blue circle) and rutile (k_{vis}(R), red circle) as a function of Γ. Rutile exhibits a higher activity than anatase because of stronger absorption of visible light. As a result of the SnO_2-surface modification, the k_{vis}(R) is almost constant, whereas the activity of anatase disappears. Although the iron oxide-surface modification of rutile was previously reported to be more effective in the visible-light-activation than anatase,[7] the reason has not been entirely clarified.

To shed light on the origin of the striking difference in the SnO_2-surface modification effect on rutile and anatase, photoluminescence (PL) spectra were measured. Figure 3 shows the PL spectra of SnO_2/anatase (A) and SnO_2/rutile (B). Anatase has a broad emission band centered at 538 nm (E_1) due to the emission from the surface oxygen vacancy levels of anatase.[10] The E_1 signal intensity significantly weakens by heating anatase at 773 K for 1 h in air, and the SnO_2-surface modification further decreases the emission intensity. Rutile has two emission bands centered at 414 nm (E_2), and 820 nm (E_3). The E_2 band is assignable to the band-to-band emission, while the E_3 band results from intrinsic defects.[24,25] In contrast to the SnO_2/anatase system, the emission intensities increase with the SnO_2-surface modification. The increase in the absorption intensity of rutile with the SnO_2-surface modification would be responsible for this feature. Further, current (I)-potential (E) curves were measured for the rutile film-coated SnO_2:F electrode (rutile/FTO) in an aerated 0.1 M $NaClO_4$ aqueous solution in the dark (Figure S3 in SI). The current due to the O_2 reduction is observed at $E < -0.2$ V, whereas only small current flows at $-0.4 < E < -0.2$ V without O_2. The O_2 reduction current increases with the SnO_2-surface modification in a similar manner as the anatase/FTO system.[1]

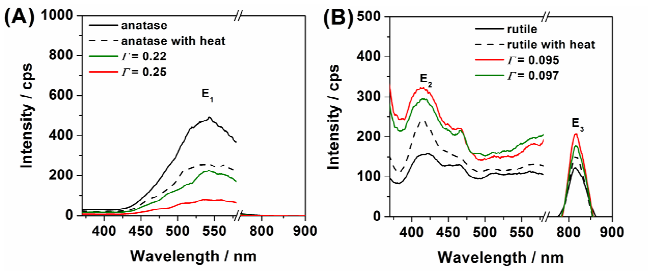

Figure 3. (A) PL spectra of SnO_2/anatase at 77 K with an excitation wavelength of 320 nm. (B) PL spectra of SnO_2/rutile measured under the same conditions.

[6] Evidently, the surface SnO_2 species promote the electron transfer from rutile to O_2.

First principles density functional theory (DFT) simulations have been undertaken on models of SnO_2 clusters adsorbed at the rutile (110) and anatase (001) surfaces. Figure 4 and 5 show the atomic structure of representative SnO_2-TiO_2 models and free SnO_2 clusters. The adsorption energies are also shown and we see that adsorption of SnO_2 clusters at either TiO_2 surface leads to a large gain in energy.

At anatase the energy gain is in the range -3.32eV to -5.29eV

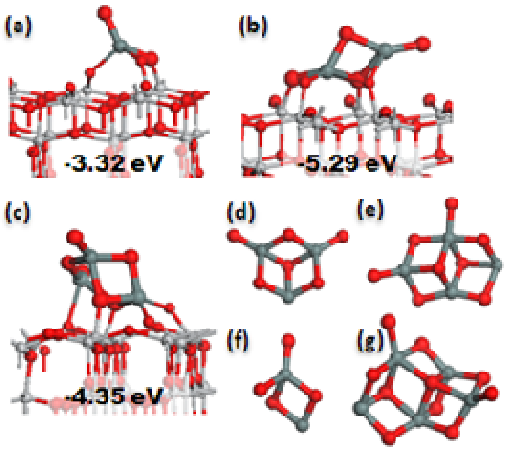

Figure 4. The atomic structure of (a) SnO_2, (b) Sn_2O_4 and (c) Sn_3O_6 clusters adsorbed at the TiO_2 (001) anatase surface. (d) – (g) show that atomic structures of free Sn_3O_6, Sn_4O_8, Sn_2O_4 and Sn_5O_{10} clusters.

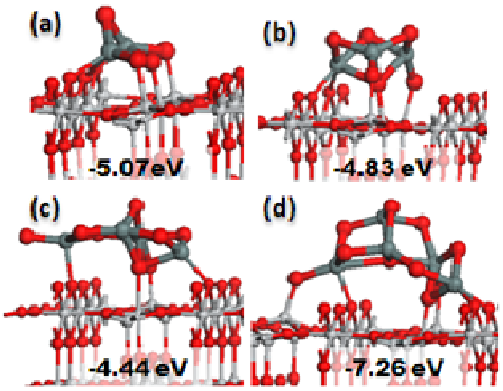

Figure 5. The atomic structures of (a) Sn_2O_4, (b) Sn_3O_6, (c) Sn_4O_8 and (d) Sn_5O_{10} clusters adsorbed at the TiO_2 rutile (110) surface.

and at rutile the energy gain is in the range of -4.44eV to -7.26eV. Examining the geometry (with detailed bond lengths given in the supporting information), SnO_2 adsorption at anatase (001) creates three new bonds, namely Sn to O atoms from the surface with distances 2.17 Å and two more bonds between cluster O atom and Ti surface atom with distances 1.78 Å and 1.77Å. Sn_2O_4 and Sn_3O_6 adsorption at anatase (001) creates five new bonds: Sn cluster and O atom surface distances are in the range 1.99 Å - 2.33 Å and the Ti-O distances for O cluster atom to surface Ti atom bonds are in the length range 1.82 Å - 1.94 Å. On anatase, we also find that SnO_2 adsorption leads to two surface oxygen atoms being pulled out of the surface to bond with cluster atoms, which is not seen with SnO_2 cluster adsorption at rutile.

At rutile (110), the Sn_2O_4 and Sn_5O_{10} clusters, which have the most negative adsorption energies, bind to the surface with seven and six new bonds respectively. Sn atoms from the cluster bond to O atoms from the surface with distances in the range 2.10 Å 2.31 Å while O atoms from the cluster create bonds to Ti surface atoms with distances which are in the range of 1.89 Å - 1.98 Å.

The clusters with less negative adsorption energies, namely Sn_3O_6 and Sn_4O_8, bond to the surface with fewer new bonds - five and four bonds, respectively. The Sn cluster atoms with O surface atoms bonds are in the range of 1.97 Å - 2.17 Å and O cluster atoms with Ti surface atoms bonds have distances ranging from 1.83 Å to 2.19 Å. All SnO_2-rutile heterostructures present a significant change in the position of the 5-fold Ti surface atoms that bind to O atoms from the cluster. The Ti atoms are displaced upwards or downwards by 0.3 Å - 0.6 Å but the bridging O atoms from rutile (110) heterostructures are not affected by interaction with the Sn cluster atoms. This is in contrast to anatase, where O atoms from the surface are pulled out of the surface layer and the Ti surface atom positions are not changed. In all heterostructures Sn atoms are 4-fold and 5-fold coordinated and O atoms in the clusters are 1, 2 and 3-fold coordinated.

To understand differences in the photocatalytic activity of SnO_2 modified rutile and anatase, we present the electronic density of states for SnO_2 modified anatase in Figure 6 and rutile in Figure 7.

On comparing the DOS, we find the following:

- For anatase, there are no SnO_2 derived states found in the band gap, with SnO_2 states lying well below the valence band (VB) and above the conduction band (CB) of anatase.
- This will lead to some enhancement of UV activity as electrons can be excited to the empty cluster states under UV light and, furthermore, these states can act as sites for O_2 adsorption and subsequent electron transfer to form reactive O_2^-.
- Figure 6 includes also Bader charge calculations results for investigated structures which indicate that the oxidation state of Sn is 4+, which is consistent with the experiment.
- For rutile, we find unoccupied SnO_2 states lying just below the rutile (110) conduction band; for example for Sn_2O_4 and Sn_4O_8 clusters, the empty SnO_2 states lie only 0.2 eV below the CB of TiO_2; for Sn_3O_6 and Sn_5O_{10} the SnO_2 states show a slightly larger offset.

The proximity of the SnO_2 states to the TiO_2 CB means that one can expect increased light absorption compared with anatase and a greater possibility for electrons to be excited to the SnO_2 states with lower energy radiation, potentially increasing the photocatalytic activity, when compared with unmodified rutile and modified anatase. However, compared with FeO_x-modified TiO_2, there is no band gap reduction.

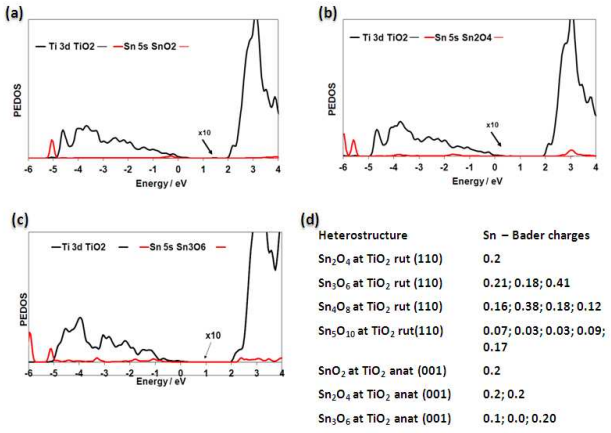

(d)

Heterostructure	Sn – Bader charges
Sn_2O_4 at TiO_2 rut (110)	0.2
Sn_3O_6 at TiO_2 rut (110)	0.21; 0.18; 0.41
Sn_4O_8 at TiO_2 rut (110)	0.16; 0.38; 0.18; 0.12
Sn_5O_{10} at TiO_2 rut(110)	0.07; 0.03; 0.03; 0.09; 0.17
SnO_2 at TiO_2 anat (001)	0.2
Sn_2O_4 at TiO_2 anat (001)	0.2; 0.2
Sn_3O_6 at TiO_2 anat (001)	0.1; 0.0; 0.20

Figure 6. Electronic density of states for Ti 3d and Sn 5s for (a) SnO_2, (b) Sn_2O_4 and (c) Sn_3O_6 modified TiO_2 anatase (001). The Bader charges on cluster Sn atoms are given in (d).

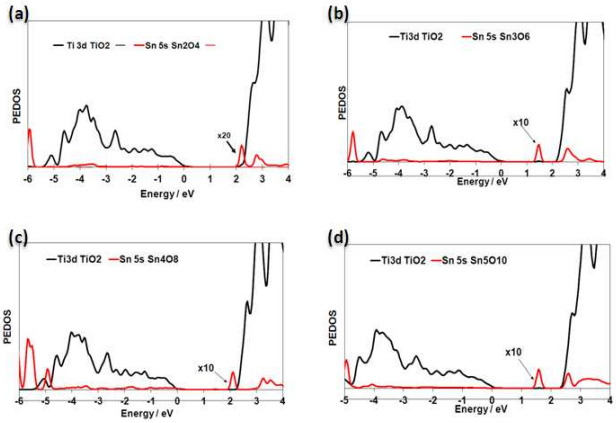

Figure 7. Electronic density of states for Ti 3d and Sn 5s for (a) $Sn2O_4$, (b) Sn_3O_6, (c) Sn_4O_8 and (d) Sn_5O_{10} modified TiO_2 rutile (110).

On the basis of the results above, the great enhancement of the UV-light-activity for rutile TiO_2 with the SnO_2-surface modification can be rationalized as follows (Scheme 1). In the oxidative decomposition of organics, the key to increase the TiO_2 photocatalytic activity is the efficient charge separation followed by the electron transfer to O_2.[26,27] The differences in interfacial Sn-O-Ti bonds of SnO_2 at rutile TiO_2 compared with anatase significantly modify the electronic structure of rutile, but not anatase. The resulting increases in the density of states near the conduction band minimum by the mixing with the SnO_2 cluster levels (Sn 5s and O2p) intensify the light absorption. The electronic transition causes bulk-to-surface interfacial electron transfer enhancing the charge separation, whereas the surface-to-bulk interfacial electron transfer occurs in the FeO_x/TiO_2[9,10] and NiO/TiO_2[11] systems. The VB edge position is invariant with the surface modification, and thus the VB-holes having a strong oxidation ability efficiently oxidize adsorbed 2-NAP without diffusion.[28] Before the immediate relaxation of the excited electrons to the conduction band minimum (or the bulk-to-surface electron transfer), O_2 is reduced with the assistance of the surface SnO_2 clusters acting as an electron transfer promoter. These cooperative effects reduce the charge recombination to greatly enhance the photocatalytic degradation of organics.

On the other hand, the electronic structure of anatase is only slightly affected by the SnO_2-surface modification, which explains the much smaller effect on its photocatalytic activity. Interestingly, Boppana and Lobo have recently shown that the SnO_x-surface modification of $ZnGa_2O_4$ by an impregnation method remarkably increases not only the UV-light-activity but also the visible-light-activity.[29] This finding also indicates that the surface modification effects strongly depend on the kind of semiconductors.

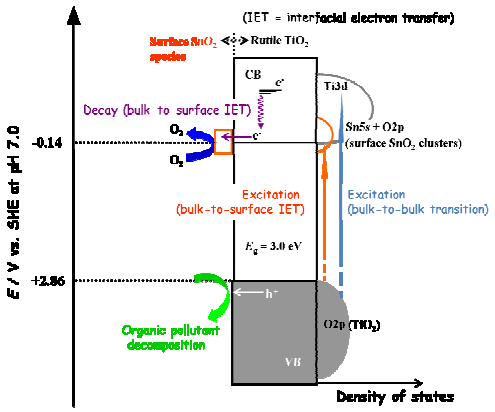

Scheme 1. Energy band diagram for SnO_2/rutile.

CONCLUSIONS

In summary, this study has shown that the SnO_2-surface modification of rutile TiO_2 leads to a great increase in its UV-light-activity, while the effect is much smaller for anatase TiO_2. DFT simulations for model clusters show that although SnO_2 clusters adsorb on both TiO_2 surfaces, the interface structure and electronic density of states present significant differences between rutile and anatase. For rutile, the changed DOS due to SnO_2 states at the CB increases light absorption and enhances charge separation. In contrast for anatase, SnO_2 states lie above the TiO_2 CB. The DFT simulation-assisted rational design for the metal oxide-surface modified TiO_2 is a promising method to develop new photocatalysts for environmental purification.

■ ASSOCIATED CONTENT

Langmuir plot of $[Sn(acac)_2]Cl_2$ on TiO_2 (Figure S1); Photocatalytic degradation of acetaldehyde (Figure S2); Dark current-potential curves in an aerated 0.1 M $NaClO_4$ aqueous solution (Figure S3). Details of the DFT simulations; structures of SnO_2 clusters adsorbed at rutile (110) and anatase (001) surfaces. This material is available free of charge via the internet at http://pubs.acs.org.

■ AUTHOR INFORMATION

Corresponding Author

*E-mail: h-tada@apch.kindai.ac.jp, michael.nolan@tyndall.ie

■ ACKOWLEDGMENTS

HT acknowledges for the financial support of Nippon Sheet Glass Foundation for Materials Science, and Engineering and by the Sumitomo Foundation. MN and AI acknowledge support from Science Foundation Ireland through the Starting Investigator Grant Program (EMOIN SFI SIRG/09/I1620), SFI-funded computational resources at Tyndall and the SFI/Higher Education Authority funded Irish Centre for High Performance Computing for the generous provision of computing resources.

■ REFERENCES

(1) Fujishima, A.; Zhang, X.; Tryk, D. A. *Surf. Sci. Rep.* **2008**, *63*, 515.

(2) Hashimoto, K.; Irie, H.;. Fujishima, A. *Jpn. J. Appl. Phys.* **2005**, *44*, 8269.

(3) Prieto-Mahaney, O. O.; Murakami, N.; Abe, R.; Ohtani, B. *Chem. Lett.* **2009**, *38*, 238.

(4) Ahmed, A. Y.; Kandiel, T. A.; Oekermann, T.; Bahnemann, D. *J. Phys. Chem. Lett.* **2011**, *2*, 2461.

(5) Irie, H.; Shibanuma, T.; Kamiya, K.; Miura, S.; Yokoyama, T.; Hashimoto, K. *Appl. Catal. B* **2010**, *96*, 142.

(6) Murakami, N.;. Chiyoya, T.; Tsubota, T.;. Ohno, T. *Appl. Catal. A.* **2008**, *348*, 148.

(7) Yu, H.; Irie, H.; Shimodaira, Y.; Hosogi, Y.; Kuroda, Y.; Miyauchi, M.; Hashimoto, K. *J. Phys. Chem. C* **2010**, *114*, 16481.

(8) Libera, J. A.; Elam, J. W.; Sather, N. F.; Rajh, T. M. Dimitrijevic, N. M. *Chem. Mater.* **2010**, *22*, 409.

(9) Tada, H.; Jin, Q.; Nishijima, H.; Yamamoto, H.; Fujishima, M.; Okuoka, S. -i.; Hattori, T.; Sumida, Y.; Kobayashi, H. *Angew. Chem. Int. Ed.* **2011**, *50*, 3501.

(10) Jin, Q.; Fujishima, M.; Tada, H. *J. Phys. Chem. C* **2011**, *115*, 6478.

(11) Jin, Q.; Ikeda, T.; Fujishima, M.; Tada, H. *Chem. Commun*. **2011**, *47*, 8814.

(12) Irie, H.; Miura, S.; Kamiya, K.; Hashimoto, K. *Chem. Phys. Lett*. **2008**, *457*, 202.

(13) Yu, H.; Irie, H.; Hashimoto, K. *J. Am. Chem. Soc*. **2010**, *132*, 6898.

(14) Liu, G.; Wang, L.; Yang, H. G.; Cheng, H. -M.; Lu, G. Q. *J. Mater. Chem.* **2010**, *20*, 831.

(15) Tada, H. *Encyclopedia of Surface and Colloid Science*, (Ed.: Hubbard, A. T.), Marcel Dekker, New York, 2002.

(16) Fujishima, M.; Jin, Q.; Yamamoto, H.; Tada, H.; Nolan, M. *Phys. Chem. Chem. Phys.* **2012**, *14*, 705.

(17) Kresse, G.; Hafner, J. *Phys Rev. B: Condens. Matter* **1994**, *49*, 1425.

(18) Perdew, J. P.; Chevary, J. A.; Vosko, S. H.; Jackson, K.A.; Pederson, M. R.; Singh, D. J.; Fiolhais, C. *Phys. Rev. B* 1993, *46*, 6671.

(19) Morgan, B. J.; Watson, G. W. *J. Phys. Chem. C* 2010, *114*, 2321.

(20) Nolan, M.; Grigoleit, S.; Sayle, D. C.; Parker, S. C.; Watson, G. W. *Surf. Sci.* 2005, *576*, 1200.

(21) Liao. P.; Carter. E. A. *J. Mater. Chem.* 2010, *20*, 6703.

(22) Nolan, M. *Phys. Chem. Chem. Phys.* 2011, *13*, 18194.

(23) Tada, H.; Matsui, H.; Shiota, F.; Nomura, M.; Ito, S.; Yoshihara, M.; Esumi, K. *Chem. Commun*. 2002, 1678.

(24) Shi, J.; Chen, J.; Feng, Z.; Chen, T.; Lian, Y.; Wang, X.; Li, C. *J. Phys. Chem.* 2007, *111*, 693.

(25) Wang, X.; Feng, Z.; Shi, J.; Jia, G.; Shen, S.; Zhou, J.; Li, C. *Phys. Chem. Chem. Phys.* 2010, *12*, 7083.

(26) Wang, C. M.; Heller, A.; Gerischer, H. *J. Am. Chem. Soc.* 1992, *114*, 5230.

(27) Hoffmann, M. R.; Martin, S. T.; Choi, W.; Bahnemann, D. W. *Chem. Rev.* 1995, *95*, 69.

(28) Irie, H.; Shibanuma, T.; Kamiya, K.; Miura, S.; Yokoyama, T.; Hashimoto, K. *Appl. Catal. B.* 2010, *96*, 142.

(29) Boppana, V. B. R.; Lobo, R. F. *ACS Catal.* **2011**, *1*, 923.

Authors are required to submit a graphic entry for the Table of Contents (TOC) that, in conjunction with the manuscript title, should give the reader a representative idea of one of the following: A key structure, reaction, equation, concept, or theorem, etc., that is discussed in the manuscript. Upon reduction, the TOC graphic should be no wider than 4.72 in. (12 cm) and no taller than 1.81 in. (4.6 cm).

The Photocatalytic Activities of Tin(IV) Oxide-Surface Modified Titanium (IV) Dioxide Show a Strong Sensitivity to the TiO_2 Crystal Form

Qiliang Jin,[a] Musashi Fujishima,[a] Michael Nolan,[b]* Anna, Iwaszuk[b], Hiroaki Tada [a]*

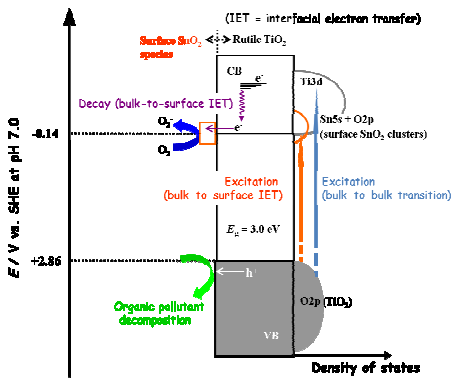

ABSTRACT FOR WEB PUBLICATION (Word Style “BD_Abstract”). Authors are required to submit a concise, self-contained, one-paragraph abstract for Web publication.

The SnO_2-surface modification of rutile TiO_2 causes a great increase in its UV-light-activity for the degradations of model organic water pollutants, while the effect is much smaller for anatase TiO_2.